An Empirical Effective Interaction for Inelastic Nucleon Scattering and Charge Exchange

Sam M. Austin

To describe inelastic scattering and charge exchange reactions in a microscopic model requires that one specify the effective two-body interaction V_{eff} between the projectile and the valence nucleons of the target. Both theoretical and empirical estimates of V_{eff} are available in the 20-50 MeV range. The theoretical estimates, based in most cases on a shell model G matrix, are quite detailed[1] but suffer from uncertainties in the bare two-nucleon interaction and in the procedures used to obtain a computationally convenient interaction from it. Moreover it is difficult to estimate these uncertainties.

The empirical interactions, on the other hand, are obtained by choosing calibration reactions sensitive only to a single spin-isospin transfer component of V_{eff} and then adjusting the strength of the selected component to match the cross section. Thus the consistency of results obtained for a variety of cases serves as a built-in measure of the uncertainty in the empirical procedure, and furthermore the empirical interaction is automatically renormalized for any systematic deficiency of the reaction mechanism. Since an earlier review of empirical information on V_{eff} was published[2], much new data has become available which bears on the isospin transfer T = 1 parts of V_{eff}. These now appear[3] to be known at least as precisely as those for T = 0.

We write the central part of the effective interaction as:

$$V_{ip}^{cent} = V_{00} + V_{10}\bar{\sigma}_i\cdot\bar{\sigma}_p + V_{01}\bar{T}_1\cdot\bar{T}_p + V_{11}(\bar{\sigma}_1\cdot\bar{\sigma}_p)(\bar{T}_1\cdot\bar{T}_p)$$
$$= V_0 + V_\sigma\bar{\sigma}_1\cdot\bar{\sigma}_p + V_T\bar{T}_1\cdot\bar{T}_p + V_{\sigma T}(\bar{\sigma}_1\cdot\bar{\sigma}_p)(\bar{T}_1\cdot\bar{T}_p).$$

where V_{ST} describes a direct amplitude with spin transfer S and isospin transfer T. Each V_{ST} is taken to have a Yukawan radial shape, with a range of 1.0 fm chosen to yield about the same mean square radius as the theoretical effective interactions.[1]

The results of the present survey for energies between 20 and 50 MeV are shown in figures 1-4. The bombarding energy is plotted on the abscissa and the strength of the 1.0 fm Yukawa interaction on the ordinent. The short horizontal lines are strengths corresponding to volume integral estimates of various theoretical potentials: the Hamada-Johnston potential (HJ), the Reid soft-core potential (R), the Kallio-Kolltveit potential (KK) and the density dependent Kallio-Kolltveit potential averaged over the lead nucleus (KKD). The numbers near the points are the masses of the targets. Results of a given experiment or analysis are denoted by a common symbol and/or connected by lines.

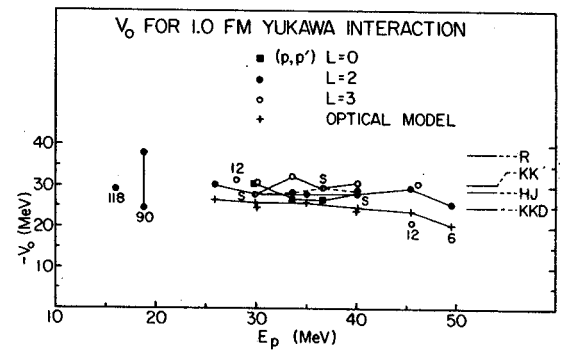

Fig. 1. Values of V_0 for real 1.0 fm range Yukawa interaction. The mean (± standard deviation) of the points is $_{16}$-27.9 ± 3.5 MeV. Points not numbered are from ^{16}O. S means two points are superimposed.

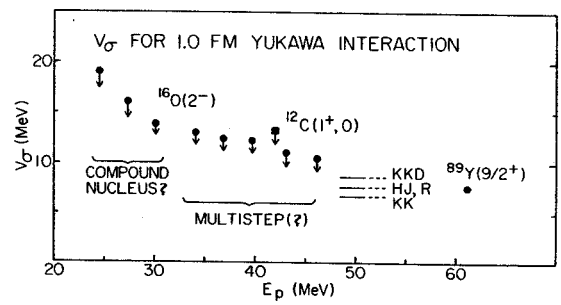

Fig. 2. Values of V_σ for a real 1.0 fm range Yukawa interaction. The downward pointing arrows indicate upper limits.

The values for V_0 and V_σ are essentially those reported earlier[2] except that in the case of V_σ it has been found[4] that the spin flip amplitude does not dominate the cross section for ^{16}O(p,p')^{16}O(2-1) so that all points based on the spin flip assumption for this reaction become upper limits. One can summarize results of figures 1-4 as:

$$V_o = -27.9 \pm 3.5 \text{ MeV}$$
$$V_\sigma = \leq 11.5$$
$$V_T = 15.2 \pm 2.2$$
$$V_{\sigma T} = 11.7 \pm 1.7$$

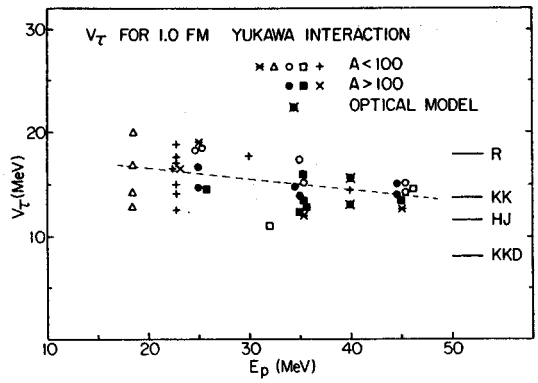

Fig. 3. Values of V_τ for a real 1.0 fm range Yukawa interaction. The mean (± standard deviation) of the points is 15.2 ± 2.2 MeV. The dashed line is drawn through the points by eye and has a slope $dV_\tau/dE_p = -0.1$.

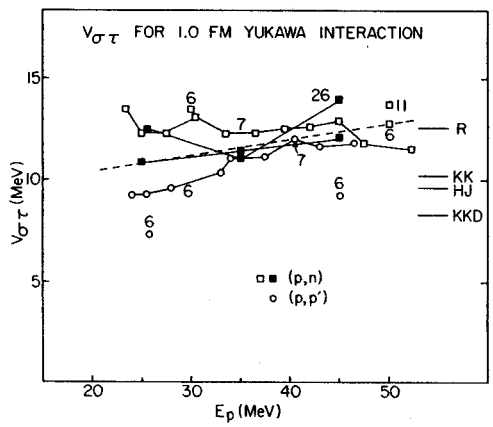

Fig. 4. Values of $V_{\sigma\tau}$ for a real 1.0 fm range Yukawa interaction. For space reasons a ^{11}B(p,n)^{11}C point, $V_{\sigma\tau}$ = 16.9 MeV at 30 MeV, has not been plotted. The mean (± standard deviation) of the points is 11.7 ± 1.7 MeV. The dashed line is drawn through the points by eye and has a slope $dV_{\sigma\tau}/dE = 0.075$.

These results imply that the interaction between two like nucleons (V^{pp} or V^{nn}) is substantially weaker than that between unlike nucleons (V^{pn}) i.e.

$$\frac{V^{pn}}{V^{pp}} = \frac{V_0 - V_\tau}{V_0 + V_\tau} = 3.4 \pm 1.2.$$

In this energy range inelastic proton scattering is then sensitive mainly to the neutron configurations of the target and comparisons with electron scattering, which is sensitive to protons, should yield the isospin structure of nuclear core excitations.[3,5]

It does not appear that it will be simple to extend this empirical procedure to high energies. Tensor and spin orbit forces are small at low momentum transfer and in most cases contribute little to inelastic scattering cross sections at bombarding energies below 50 MeV. The central force then dominates the cross section and one can isolate individual v_{ST}. At energies above 100 MeV on the other hand, the tensor and spin orbit forces are important in most cases. It then becomes difficult to isolate individual terms in V_{eff} and it seems unlikely that the empirical procedure will be as useful as it is at lower energies.

More details concerning this empirical interaction can be found in Ref. 3.

---

1. G. Bertsch, J. Borysowicz, H. McManus and W.G. Love, Nucl. Phys. A284, 399 (1977).
2. S.M. Austin, pg. 285 in The Two Body Force In Nuclei, ed. by S.M. Austin and G.M. Crawley, (Plenum, New York, 1972)/
3. S.M. Austin, Proceedings of the Telluride Conference on the (p,n) reaction and the Nucleon-Nucleon Force, to be published.
4. J.M. Moss, W.D. Cornelius and D.R. Brown, Phys. Rev. Lett. 41, 930 (1978).
5. D. Larson, S.M. Austin and B.H. Wildenthal, Phys. Rev. C11, 1638 (1975).

Inelastic Proton Scattering on ^{194,196,198}Pt

P.T. Deason, R.M. Ronningen, C.H. King,* T.L. Khoo,** F.M. Bernthal and J.A. Nolen, Jr.

We are investigating the (p,p') reaction at 35 MeV on ^{194,196,198}Pt in conjunction with our (p,t) reaction studies[1] on these same nuclei. Precise energy levels in ^{198}Pt are now being extracted; 38 of the 44 levels observed (to 3.2 MeV in excitation) are seen for the first time. These data were recorded on a nuclear emulsion plate in the focal plane of the Enge split-pole magnetic spectrograph at $\theta_{lab}=43^{o}$ (chosen to minimize interfering contaminant reactions). Two calibrating reactions, ^{196}Pt and ^{206}Pb (p,p') were recorded on the same plate. The resolution is about 7 keV FWHM. The assignment of new levels with good precision (2-4 keV) in ^{196}Pt could also be made by using the internal, well-known level energies. Figure 1 shows the plate data for the ^{194,196,198}Pt (p,p') reactions. By using empirical angular distribution shapes for states of known J^{π}, we are attempting to deduce J^{π} assignments for the new levels observed in each reaction.

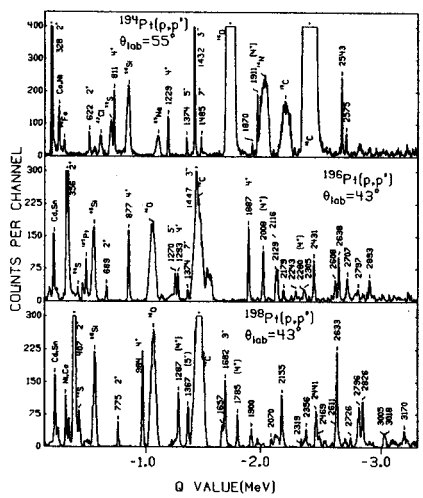

Fig. 1. Plate data used for calibrating the ^{194,196,198}Pt(p,p') reactions. '*' means that peak has been cut off at maximum value on vertical scale or was unscannable.

We are also performing coupled channels calculations to describe the excitations of the 0^{+}, 2^{+}, 4^{+}, $2^{+}{}'$, and $4^{+}{}'$ states. We are using the coupled channels code ECIS[2] and presently a symetric rotor model in which the magnitudes and signs of the relative matrix elements are taken from the IBA model, which has quite successfully reproduced several spectroscopic features of the Pt nuclei observed in γ-spectroscopy studies[3] and in our (p,t) studies.[1] We find that good fits to our data can be obtained within this framework. The best fits result when the sign of P_3 ($P_3 = M_{02'}$, $M_{22'}$, M_{02}) is negative for ^{194,196,198}Pt which is in agreement with α-scattering results[4] (see Fig. 2). We find in each nucleus the data for the $4^{+}{}'$ state are underestimated by the calculation in which this state is excited by mainly two- and three-step excitations. As shown in Figure 3, we find substantial improvements if we include a direct E4 excitation of the $4^{+}{}'$ state. The values of M_{04}, which fit best the data are about 75% those to the 4^{+} members of the ground band. However, these values are not absolute but relative to the assumptions of signs and magnitudes of the matrix elements of the competing paths of excitation.

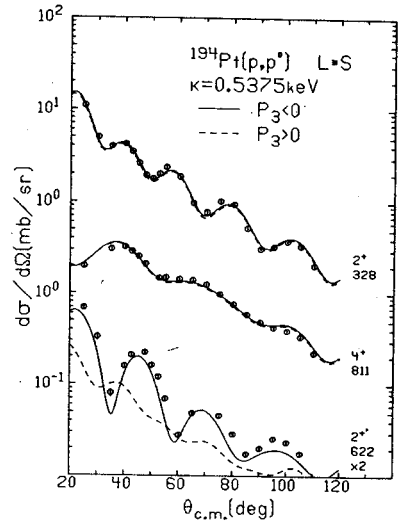

Fig. 2. Data and 0-2-4-2' ECIS calculations for ^{194}Pt with spin-orbit interaction. $\beta_2=-0.151$, $\beta_4=-0.0453$.

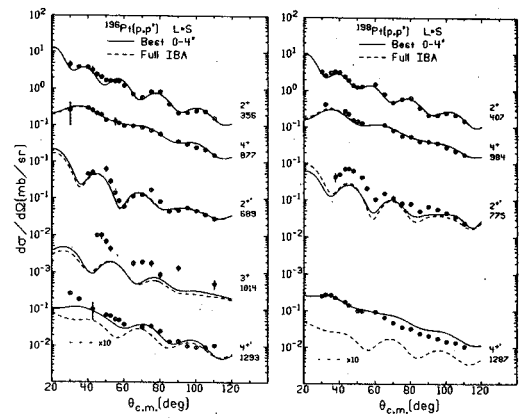

Fig. 3. Data and 0-2-4-2'-3-4' ECIS calculations for ^{196,198}Pt (The 3+ level was not included for ^{198}Pt). The dashed curves used a full set of 0(6) IBA matrix elements, while the solid curves are the result of a search on the 0-4+' E4 matrix element.

We have calculated the E2 and E4 moments from the parameters of the deformed optical model potentials. These are shown in Figure 4 and are compared to values from other studies.

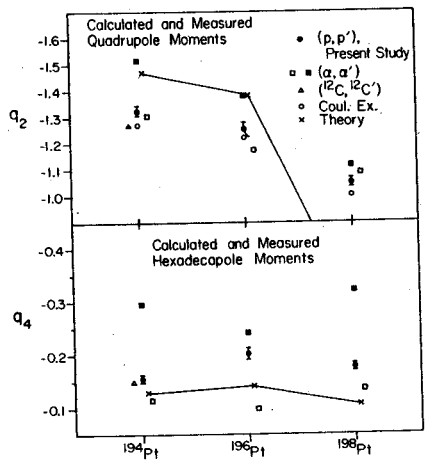

Fig. 4. Quadrupole and hexadecapole moments for ^{194,196,198}Pt. (α,α') from reference 4, $(^{12}C,^{12}C')$ - F.T. Baker et al., Nuc. Phys. A321, 222 (1979), Coul. Ex.-C. Baktash et al., Phys. Rev. C18, 131 (1978); J.E. Glenn et al., Phys. Rev. 188, 1905 (1969); Theory - U. Gotz et al., Nucl. Phys. A192, 1 (1972). The units are b or eb, for q_2, and b^2 or eb^2, for q_4.

---

* Bell Laboratories, Murray Hill, NJ
** Physics Division, ANL, Argonne, IL

1. P.T. Deason et al., to be published, Phys Rev. C20, 1979.
2. ECIS, unpublished, written by J. Raynal.
3. J.A. Cizewski et al., Phys. Rev. Lett. 40, 167 (1978).
4. F.T. Baker et al., Nucl. Phys. A266, 377 (1976).

Quadrupole and Hexadecapole Moments in Lanthanide and Actinide Nuclei from Proton Inelastic Scattering

R.M. Ronningen, R.C. Melin, J.A. Nolen, Jr., G.M. Crawley, C.H. King, J.E. Finck, and C.E. Bemis, Jr *

Because the nuclear interaction is poorly understood and is much more complicated than the electromagnetic interaction, it is difficult to make model-independent determinations of nuclear shapes from measurements of inelastic scattering cross sections. For simplicity it is usual to analyze the data in terms of a parametrized deformed optical model optential (DOMP), which is a complex projectile-nucleus potential as in the normal optical model but with additional parameters describing the deformation of the nuclear surface. The parameters are then adjusted to fit both the elastic and inelastic scattering cross sections. The phenomenological nature of this model makes the deformation parameters (β_λ) determined by such an analysis rather uncertain and difficult to compare with Coulomb excitation results. Recently, Mackintosh[1] has pointed out that deformed optical model potentials which are derivable from a simple folding prescription (sometimes called the reformulated optical model) have the property that their multipole moments are proportional to those of the underlying matter distribution.[2] Thus, to the extent that the DOMP satisfies this property, the moments of the mass distribution can be determined in a model-independent way. The purpose of our study is to provide (p,p') data so that the possible advantages of proton scattering as a probe of nuclear deformations and mass distributions can be assessed. We are now analyzing data from 35 MeV proton inelastic scattering on $^{152,154}Sm$, ^{154}Gd, ^{176}Yb, ^{180}Hf, ^{186}W, ^{232}Th, and $^{234,236,238}U$. During this past year we have submitted for publication[3] the first results of our study of ^{154}Sm, ^{176}Yb, ^{232}Th, and ^{238}U. The optical model and deformation parameters for coupled channel calculations from this study are summarized in Table I. The quadrupole and hexadecapole "charge" moments from these optical model parameters are presented in Table II along with moments deduced in Coulomb excitation,[4,5] electron scattering,[6] and α-particle scattering studies.[7,8,9] We find the moments from our study to agree better with those from Coulomb excitation than with moments deduced from α-particle scattering. But, we also find the moments from our study to be systematically smaller than those from Coulomb excitation. If the systematic difference is not a result of the phenomenological aspects of our analysis, then this might imply smaller neutron distribution moments than proton moments, this disagreeing with Hartree-Fock calculations[10] for ^{232}Th and ^{238}U.

In order that ^{154}Sm, ^{176}Yb, ^{232}Th, and ^{238}U become better test cases for our continuing analysis, we have since taken more complete angular distribution data, which now, at least for the ground and 2^+ states, span the angular range of 20° to $\lesssim 144.5^\circ$ in 2.5° steps. To obtain the data backwards of 120° (and some data inwards to 90°)

Table I. Optical model parameters for coupled channels calculations.

		V^a (MeV)	a_r (fm)	$W_d{}^b$ (MeV)	a_i (fm)	$V_{so}{}^c$ (MeV)	β_2	β_4
^{154}Sm	d	50.70	0.729	5.113	0.686	6.330	0.269 (3)	0.072 (3)
	e	49.80	0.667	8.392	0.604		0.273 (5)	0.066 (5)
^{176}Yb	d	52.45	0.705	4.204	0.738	6.430	0.275 (4)	-0.055 (4)
	e	49.67	0.652	7.745	0.653		0.277 (7)	-0.066 (6)
^{232}Th	d	52.72	0.716	5.086	0.788	5.513	0.210 (3)	0.069 (3)
	e	51.70	0.707	7.085	0.759		0.211 (4)	0.071 (3)
^{238}U	d	53.59	0.732	4.331	0.810	6.776	0.232 (3)	0.042 (3)
	e	52.15	0.653	6.121	0.789		0.233 (4)	0.049 (5)

[a]The real radius was kept fixed at $r_r = 1.17$ fm.
[b]The imaginary radius was kept fixed at $r_i = 1.32$ fm.
[c]The spin-orbit geometry parameters were kept fixed at $r_{so} = 1.01$ fm and $a_{so} = 0.750$ fm.
[d]These parameters resulted from best-fits for calculations which included the spin-orbit interaction.
[e]These parameters resulted from best-fits for calculations not employing a spin-orbit interaction.

Table II. E2 and E4 moments in ^{154}Sm, ^{176}Yb, ^{232}Th, and ^{238}U.

Nuclide	Method	q_2 [a] (b) or (eb)	q_4 [a] (b^2) or (eb^2)
^{154}Sm	(p,p')	2.06 (3)	0.54 (2)
	at 35 MeV[b]	2.05 (5)	0.49 (3)
	Coulomb excitation[c]	2.094 (4)	0.588 (29)
	(e,e')[d]		|0.47| (1)
	(α,α')	2.38	0.61
	at 50 MeV[e]		
^{176}Yb	(p,p')	2.29 (5)	-0.09 (3)
	at 35 MeV[b]	2.26 (8)	-0.13 (5)
	Coulomb excitation[c]	2.325 (18)	0.28 ($^{11}_{20}$)
	(e,e')[d]		|0.10|
	(α,α')	2.76	-0.17
	at 50 MeV[e]		
^{232}Th	(p,p')	2.93 (6)	0.98 (5)
	at 35 MeV[b]	2.94 (7)	1.00 (5)
	Coulomb excitation[f]	3.03 (1)	1.22 (15)
	(e,e')[d]		|1.08| (2)
	(α,α')	2.97 (21)	1.06 (20)
	at 50 MeV[g]		
^{238}U	(p,p')	3.30 (6)	0.81 (6)
	at 35 MeV[b]	3.29 (8)	0.84 (7)
	Coulomb excitation[f]	3.51 (2)	0.83 (22)
	(e,e')[d]		|1.10| (3)
	(α,α')	2.98 (12)	0.74 (8)
	at 50 MeV[g]		
	(α,α')	3.75 (22)	1.42 (27)
	at 50 MeV[h]		

[a] The units for the charge component moments are b^λ, λ = 2 or 4. The units for the electromagnetic moments are eb^λ.

[b] Present work using the values of the parameters in Table I with spin-orbit interaction. Calculations without spin-orbit interaction yield the following changes in q_2: -0.01, -0.03, +0.01, and -0.01 b, and in q_4: -0.05, -0.04, +0.02, +0.03 b^2 for ^{154}Sm, ^{176}Yb, ^{232}Th, and ^{238}U, respectively.

[c] The Coulomb excitation values for q_2 and q_4 are results of the survey of Ref. 4.

[d] Ref. 6. "||" denotes the absolute value of the enclosed number.

[e] Ref. 8.

[f] Ref. 5.

[g] Ref. 9.

[h] Ref. 7.

the technique[11] for dispersion-matching in a reflective beam-target geometry was employed. Fig. 1 indicates the quality of these data for ^{154}Sm. The additional 6^+ state data will be especially important to the test of the sensitivity of proton inelastic scattering at 35 MeV to the effects of the β_6 deformation.

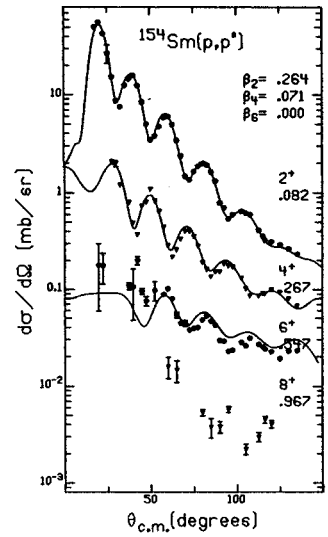

Fig. 1

The newer data taken on ^{152}Sm, ^{154}Gd, ^{180}Hf, ^{186}W, and $^{234,236,238}U$ will provide several complimentary tests of results from other experimental methods. The N = 90 isotope ^{154}Gd has[4] possibly the largest positive β_4 value in the rare-earth region. With its low-lying, collective $K^\pi = 0^+$ and 2^+ bands, it will also provide a test of the coupled channels analysis of vibrational state excitations.

The nuclides ^{180}Hf and ^{186}W have[4] possibly large, negative values of β_4. Fig. 2 shows a preliminary coupled channels analysis of the ^{180}Hf data indicating that indeed this nucleus has a value of β_4 which is substantially negative. A qualitative feature of the 4^+ data for a large, negative β_4 value is the lack of a pronounced diffractive structure; this is also observed for the Pt nuclei[12] which have $\beta_4 < 0$. The cross sections for the 6^+ state excitations are overestimated when β_2 and β_4 are so large, and when $\beta_6 = 0$.

The data on the three isotopes of U will allow us to check the trends[5,9] of the quadrupole and hexadecapole moments in this mass region as previously determined by Coulomb excitation[5] and α-particle inelastic scattering.[9]

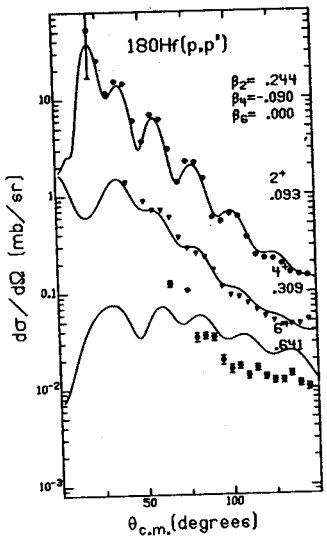

Fig. 2

* Oak Ridge National Laboratory, Oak Ridge, TN 37830.

1. R.S. Mackintosh, Nucl. Phys. A266 (1976) 379.
2. G.R. Satchler, J. Math. Phys. 13 (1972) 1118.
3. C.H. King et al., accepted for publication in Phys. Rev. C.
4. For a compilation of E2 and E4 moments from Coulomb excitation in the lanthanide region, see R.M. Ronningen et al., Phys. Rev. C16, (1977) 220.
5. C.E. Bemis, Jr. et al., Phys. Rev. C8 (1973) 1446.
6. T. Cooper et al., Phys. Rev. C13 (1976) 1083.
7. D.L. Hendrie, Phys. Rev. Lett. 31 (1973) 478.
8. D.L. Hendrie, et al., Phys. Lett. 26B (1969) 12.
9. B. David et al., Z. Physik A278 (1976) 281.
10. J.W. Negele and G. Rinker, Phys. Rev. C9 (1977) 1499 and J.W. Negele, private communication.
11. See R.C. Melin et al., this Annual Report.
12. See P.T. Deason et al., this Annual Report.

Energy Dependence in the $^{92}Mo(p,p')^{92}Mo^*$ Reaction

R.A. Moyer,[†] R.W. Finlay,[+] and G.M. Crawley

Recent studies[1] of inelastic scattering of fast neutrons from single-closed-shell nuclei have provided strong evidence of an explicit isospin dependence of nuclear deformation parameters. The magnitude and sign of the observed isospin dependence is in good agreement with earlier theoretical predictions,[2] and it has been possible, in some cases, to extract isoscalar and isovector deformation parameters of quadrupole states.[3,4]

The determination of isovector deformation parameters is sensitive to the small (< 20%) differences between deformation parameters measured in (n,n') and (p,p') reactions. It is therefore essential that these reactions be measured with good accuracy and that the data be analyzed in the same framework. In Refs. 1, 3, and 4, new measurements of neutron inelastic scattering were compared with proton scattering measurements in the literature. The method suffers from the obvious drawback that proton scattering experiments with the same target nucleus are not always in good agreement with each other. Moreover, there are suggestions throughout the literature that the deformation parameters measured in proton inelastic scattering are not constant. The values have a tendency to decrease with increasing bombarding energy and the effect is especially pronounced for states of high angular momentum. The existence of such an effect would, of course, confound the comparison of proton and neutron scattering since the experiments are not always performed at the incident energy appropriate to such a comparison.

The purpose of this investigation was to search for an explicit energy dependence of the collective-model deformation parameters for a single-closed-shell nucleus over the energy range from 25 to 45 MeV. The nucleus ^{92}Mo was chosen for several reasons: the neutron data already existed for ^{92}Mo but the existing data on $^{92}Mo(p,p')$ showed significant discrepancies, the spectrum of low-lying states in ^{92}Mo also contains a number of widely-spaced normal parity states which can be described in the collective model. Differential elastic and inelastic scattering cross sections were measured for ^{92}Mo over a range of scattering angles from $\theta \cong 10°$ to $\theta \cong 120°$ for incident proton energies of 25, 30, 35, 40, and 45 MeV. Special attention was given to the measurement at 35 MeV where no previous measurements were available. Protons were detected in a position-sensitive proportional counter at the focal plane of the Enge magnetic spectrometer with an overall energy resolution of 25 keV which was perfectly adequate for this experiment.

Elastic scattering cross sections were analyzed in terms of an optical model which contained both volume- and surface-absorption terms. Spin-orbit potential parameters were held fixed at the values quoted by Becchetti and Greenlees.[6] Real and imaginary well depths and geometrical parameters were searched, starting with the values of Becchetti and Greenlees, with the optical model code GENOA.[7] The geometrical parameters which were obtained from these searches were averaged to provide a fixed (energy independent) set and the code GENOA was used again to search for the potential depths which best fit the elastic scattering data within this constraint of fixed geometry. The fits to the elastic scattering data were satisfactory at 25, 30, 35, and 45 MeV. The data set at 40 MeV was not complete enough to warrant further analysis.

The distorted-wave code DWUCK[8] was used to calculate the inelastic scattering cross sections within the framework of the collective model. The fixed-geometry optical model parameters were used for these calculations. Deformation parameters were obtained for the first five eigenstates in $^{92}Mo(J^\pi = 2^+, 4^+, 5^-, 3^-, 2^+)$ at each of four bombarding energies. Preliminary results for the deformation parameters are shown in the table.

A first glance at the table shows that for all five eigenstates, the deformation parameters are constant within the quoted errors from E_p = 30 to 45 MeV. It is also evident that for all five eigenstates, the parameters obtained at 25 MeV are larger than those obtained at the higher energies. A recent study of the $^{92}Mo(p,p')$ reaction at 20 MeV[9] is in agreement with this trend in that the deformation parameters obtained at 20 MeV are larger than our 30-45 MeV values for all five states and larger than our 25 MeV values in four of the five cases.

Further investigations are in progress to ascertain the effects of optical model parameterization on extracted deformation parameters throughout this energy region.

[†]Department of Nuclear Engineering, Univ. of Wisconsin, Madison, Wisconsin.

[+]Ohio University.

1. D.E. Bainum et al., Phys. Rev. Lett. 39, 443 (1977).

2. V.A. Madsen, V.R. Brown, and J.D. Anderson, Phys. Rev. Lett. 34, 1388 (1975) and Phys. Rev. C12, 1205 (1975).

3. D.E. Bainum et al., Nucl. Phys. A311, 492 (1978).

4. R.W. Finlay et al., Phys. Lett. 84B, 169 (1979).

5. See, for example, R.A. Hinrichs et al., Phys. Rev. C7, 1981 (1973), W.T. Wagner, G.M. Crawley, G.R. Hammerstein, and H. McManus, Phys. Rev. C12, 757 (1975).

6. F.D. Becchetti, Jr. and G.W. Greenlees, Phys. Rev. 182, 1190 (1969).

7. F.G. Perey, private communication (1974).

8. P.D. Kuntz, University of Colorado, unpublished.

9. E.J. Kaptein, thesis, Vrije Universiteit, Amsterdam (1978), unpublished.

Table 1. Deformation parameters and lengths.

Incident Energy (MeV)	2^+ (1.5094 MeV) β_L	δ_L[†]	4^+ (2.2825 MeV) β_L	δ_L[†]	5^- (2.5262 MeV) β_L	δ_L[†]	3^- (2.8487 MeV) β_L	δ_L[†]	2^+ (3.092 MeV) β_L	δ_L[†]
25	.093 ± .009	.492 ± .048	.064 ± .005	.339 ± .026	.079 ± .009	.418 ± .048	.154 ± .020	.815 ± .106	.050 ± .006	.265 ± .032
30	.082 ± .007	.434 ± .037	.058 ± .009	.307 ± .048	.063 ± .008	.334 ± .042	.132 ± .020	.699 ± .106	.043 ± .006	.228 ± .032
35	.083 ± .008	.440 ± .042	.059 ± .006	.312 ± .032	.066 ± .006	.408 ± .032	.136 ± .006	.720 ± .032	.040 ± .004	.212 ± .021
45	.079 ± .010	.418 ± .053	.057 ± .007	.302 ± .037	.063 ± .009	.397 ± .048	.135 ± .013	.715 ± .069	.041 ± .007	.217 ± .037

[†] δ_L = the deformation length = $\beta_L R_R$, units are fm.

The ^{26}Mg(p,n) Reaction and Values of $V_{\sigma\tau}$ and V_{τ}

W.A. Sterrenburg, S.M. Austin, U.E.P. Berg, and R.P. DeVito

The ^{26}Mg(p,n) reaction has been studied at bombarding energies of 25, 35, and 45 MeV. Angular distributions were measured at angles between 10^{o} and 100^{o} with the MSU beam swinger and 2 neutron detectors, a 12.7 cm diameter x 7.6 cm long cyclindrical cell filled with NE 213 scintillator liquid and a 84 x 13 x 2.5 cm^3 rectangular box containing NE 224. The detectors were placed at 14.0, 22.5, and 33.8 meters, depending on the required resolution at the different bombarding energies. The target was 5 mg/cm^2 thick and enriched to 99% in ^{26}Mg. The beam current was typically 1 μA on target. Fig. 1 shows a neutron time-of-flight (TOF) spectrum measured at E_p = 25 MeV and $\theta_n = 25^{o}$ with a flight path of 22.5 m. The energy resolution for the isobaric analog state (IAS) at E_x = 0.228 MeV in ^{26}Al for that case is about 140 keV.

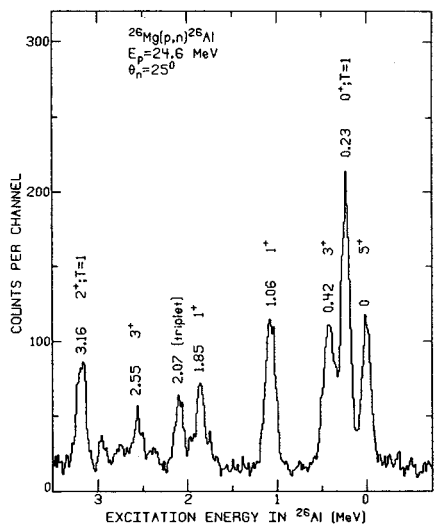

Fig. 1. Neutron time-of-flight spectrum from the (p,n) reaction on ^{26}Mg. The flight path was 22.5 m.

The study was carried out to obtain useful values for parameters describing the effective interaction between the incident protons and the target nuclei. The central part of this nucleon-nucleon force is usually parameterized as

$$V_o + V_\sigma \vec{\sigma}_i \cdot \vec{\sigma}_p + V_\tau \vec{\tau}_i \cdot \vec{\tau}_p + V_{\sigma\tau} (\vec{\sigma}_i \cdot \vec{\sigma}_p)(\vec{\tau}_i \cdot \vec{\tau}_p),$$

in which i and p stand for target nucleon and projectile, respectively. In the ^{26}Mg(p,n) case $V_{\sigma\tau}$ dominates the transition to the first 1^+ state in ^{26}Al at E_x = 1.058 MeV because a spin flip takes place, whereas the reaction to the IAS only involves a charge exchange and is thus predominantly described by V_τ. All four components of the central force were calculated for a 1 fm range Yukawa interaction. V_o has been well established[1] and was fixed at -27 MeV in the present analyses. The value for V_σ is less certain but was kept at 9 MeV, as was done in a similar analysis of the ^{7}Li(p,n) reaction.[2] The transition densities used in the DWBA calculations are from a full sd-shell model study of Chung and Wildenthal.[3]

We obtained values for V_τ and $V_{\sigma\tau}$ by matching the predicted total cross sections over the measured angular range with the experimental cross sections for the 0^+; T=1 and 1^+; T=0 states, respectively. The measured angular distributions and the DWBA predictions are shown in Fig. 2. Included in the calculations shown is a non-central component of the form

$$V_{T\tau} \; r^2 \; \frac{e^{-r/\mu}}{r/\mu} \; S_{12} \; \vec{\tau}_i \cdot \vec{\tau}_p$$

in which S_{12} is the tensor operator, μ=0.816 μm and $V_{T\tau}$ was set at 7 MeV/fm^2. The deduced values for V_τ and $V_{T\tau}$ and the ratios $V_{\sigma\tau}/V_\tau$ are listed in Table I. All values agree reasonably well with values for other nuclei at various bombarding energies.[1] The ratio $V_{\sigma\tau}/V_\tau$ increases with increasing energy. This follows the trend of results obtained by Goodman[4] and Love[5] for higher energies.

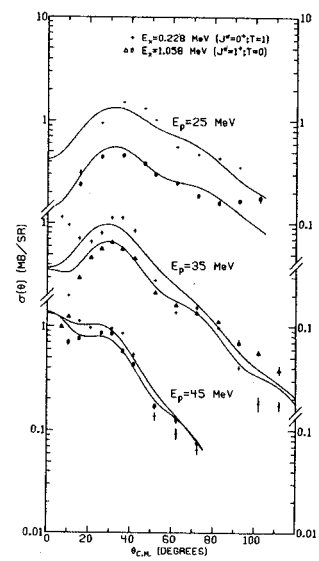

Fig. 2. Angular distributions and DWBA fits for the first 0^+; T=1 and 1^+; T=0 states in ^{26}Al at three different bombarding energies.

Table I. V_τ and $V_{\sigma\tau}$ at different bombarding energies.

E_p (MeV)	V_τ (MeV)	$V_{\sigma\tau}$ (MeV)	$V_{\sigma\tau}/V_\tau$
24.6	17.9	13.3	0.74
35.0	11.6	11.5	0.99
45.0	10.5	11.4	1.09

1. S.M. Austin, Telluride Conference (1979).
2. L.E. Young et. al., MSU Cyclotron Laboratory Annual Report 1977-1978.
3. W. Chung and B.H. Wildenthal, private communication.
4. C. Goodman, Telluride Conference (1979).
5. W.G. Love, Telluride Conference (1979).

Evidence for isovector giant resonances in the continuum of (p,n) reactions on isotopes from ^{90}Zr to ^{208}Pb

W.A. Sterrenburg, S.M. Austin, R.P. DeVito and A.I. Galonsky

INTRODUCTION

Many of the studies with (p,n) reactions at sufficiently high bombarding energies have been focused on the properties of isobaric analog ground states (IAS), mainly because these non spin-flip transitions are the most dominant features in many (p,n) reactions observed and were useful for instance in obtaining a reliable set of optical model parameters.[1,2]

More recently another feature of the (p,n) reaction was observed, first[3] in the ^{90}Zr(p,n) case: a broader (about 4 MeV FWHM) structure not far above the IAS. This was interpreted as the predicted[4] giant Gamow-Teller or spin-flip transition. The present work was done to study this transition in more detail. The (p,n) reaction seemed very suitable for this study because of the selectiveness of the mechanism to isovector states; no isoscalar resonances can be excited, resonances which can easily obscure the effects one is interested in.

EXPERIMENT

As a follow-up of the observation of cross section enhancements in the neutron spectrum of the ^{90}Zr(p,n) reaction we have done (p,n) reactions on $^{90,91,92,94,96}Zr$, as well as on $^{94,96,97,98,100}Mo$, $^{112,116,120,122,124}Sn$, ^{93}Nb and ^{208}Pb. For that purpose a 45 MeV proton beam from the MSU cyclotron was focused on those targets. Outgoing neutrons were detected in a 5 inch diameter x 3 inch long cylindrical cell, filled with NE 213 scintillator liquid, placed at a distance of 7 meters from the target. Signals originating from γ-rays were separated from those caused by neutrons with pulse shape discrimination, described in more detail in ref. 5. Typical beam currents were 1.5 μA on target. Target thicknesses ranged from 1 to 10 mg/cm^2. All signals were routed into a sigma-7 computer for direct on line monitoring.

RESULTS AND INTERPRETATION

Figure 1 shows neutron time-of-flight spectra for various targets at a detection angle of 7.5°. The broad structure near the IAS is present in all cases. Like for the IAS their positions do not depend on the ground state Q-values, which leads to the conclusion that they too are analogs of states in the target nuclei, possibly of concentrated M1 states. Another broad enhancement at higher excitation energy had been observed[6] both in the $^{90}Zr(^3He,t)$ and in the ^{90}Zr(p,n) reaction. This feature is less noticable in the spectra in Fig. 1, but also the position of this bump is almost independent of the target material and therefore they must be analogs of states in the target nucleus as well.

One of the most likely explanations for the enhancement near the IAS is the following. Consider the ^{90}Zr(p,n) case (see Fig. 2). The analogs of the 1^+; T=5 states in ^{90}Zr can be constructed by application of the isospin lowering operator. In this way a 2p-2h and a 1p-1h wave function are obtained with weights of $\sqrt{9/10}$ and $\sqrt{1/10}$, respectively. Since only the 1p-1h component can be reached in a direct (p,n) reaction the cross section for this analog state is not expected to be very high. The anti-analog state, however, constructed from the orthonormal wave function is expected to have a larger cross section because now the 1p-1h part has the larger coefficient. In addition the angular distribution is consistent with the simultaneously measured distribution for known isolated 1^+ states.

For the upper bump the situation is less straight forward. Two explanations will be discussed. First the hypothesis[6] that it is the analog of the M1 state in the target nucleus. Its measured Q-value (-27 MeV) would imply an excitation energy of the M1 state in ^{90}Zr of 15 MeV, which is way above the predicted[7] 9 MeV, based on a 40 $A^{-1/3}$ dependence of the M1 excitation energy on the mass number A. A second possible explanation is that the higher bumps are the anti-analogs of the giant E1 resonances in the target nuclei. The position of the E1 resonance is well known in ^{90}Zr and lies at E_x = 16.8 MeV. The isospin splitting will bring it about 3.5 MeV down in ^{90}Nb, so 13.3 MeV above the IAS at 5.1 MeV. This would correspond exactly with the measured position of the bump. Its angular distribution, however, is more consistent with a 1^+ than a 1^- assignment. Our hypothesis at this moment is that the bumps are anti-analog of M1 and E1 states. Careful analyses of the Q-value systematics of the cross section enhancements for all the isotopes studied is in progress. Also measurements at much higher energies (100-150 MeV), where one expects a better peak-to-background ratio because the spin-flip strength is found[8] to be enhanced over the non spin-flip strength, may shed some light on the problem.

---

1. J.D. Carlson, C.D. Zafiratos and D.A. Lind, Nucl. Phys. A249, 29 (1975).
2. D.M. Patterson, R.R. Doering and Aaron Galonsky, Nucl. Phys. A263, 261 (1976).
3. R.R. Doering, Aaron Galonsky, D.M. Patterson and G.F. Bertsch, Phys. Rev. Lett. 35, 1691 (1975).

4. K. Ikeda, S. Fujii, and J.I. Fujita, Phys. Lett. 3, 271 (1963).
5. R. St. Onge, Aaron Galonsky, R.K. Jolly, and T.M. Amos, Nucl. Instr. and Meth. 126, 391 (1975).
6. Aaron Galonsky, J.P. Dideliz, A. Djaloeis, and W. Oelert, Phys. Lett. 74B, 176 (1978).
7. L.W. Fagg, Rev. Mod. Phys. 47, 683 (1975).
8. W.G. Love, Telluride Conference 1979.

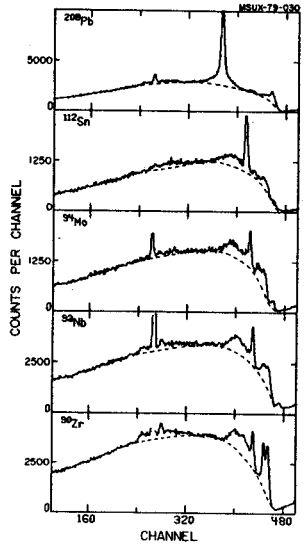

Fig. 1. Neutron time-of-flight spectra for five targets measured at θ_n=7.5° showing the broad cross section enhancements on a continuum background.

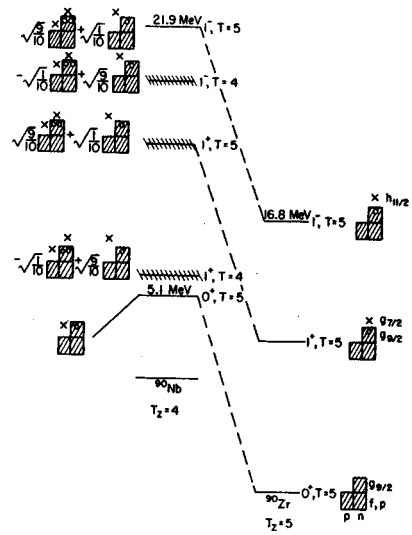

Fig. 2. Giant resonance states of ^{90}Zr and their isobaric analogs and antianalogs in ^{90}Nb.

Elastic Scattering of ^{6}Li at 73.7 MeV

R. Huffman[+], A. Galonsky, R. Markham[++] and C. Williamson[+++]

Angular distribution for ^{6}Li elastic scattering at 73.7 MeV from targets of ^{58}Ni, ^{90}Zr, ^{124}Sn, and ^{208}Pb have been measured. The optical-model parameters for Woods-Saxon real and imaginary volume potentials have been found which describe the data well and exhibit both discrete and continuous ambiguities.

The results of extensive searches on the ^{58}Ni data are shown in Fig. 1. The parameters of the five X^2 minima, designated Families I through V, are listed in the table. There are, of course, even more solutions. Figure 2 demonstrates the ambiguity by showing fits to the data for three of the families. From Fig. 3 we see that the common feature of the real potential wells is the surface region. Strong absorption makes the interior of the well irrelvant to the scattering. Similar results have been obtained for the other targets in this study: ^{90}Zr, ^{124}Sn, and ^{208}Pb.

In order to seek optical-model parameters which vary smoothly across the periodic table, searches were performed in which a fixed geometry was imposed. For each target only the well depths, V_R and W_S, were varied. Five different fixed geometries were used, namely the geometries of Families I through V, which resulted from searches on the Ni data. Hence, only the Zr, Sn, and Pb data remained to be searched on. The manner of holding the radius part of the geometry fixed depends, however, on definition. In the light-ion convention the radius of the well for the target of mass number A is defined as $r_o A^{1/3}$, where r_o is fixed for all A. (There are, of course, two values of r_o, one for the real well and one for the imaginary well.) The values used for r_o were those listed in the table. The resulting values of V_R and W_S are plotted in Fig. 4 and fitted with straight lines. This parameterization appears reasonably appropriate and should permit interpolation and extrapolation to obtain optical-model parameters for targets other than the four studied here. In the heavy-ion convention the radius is defined as $r_o' (A^{1/3} + 6^{1/3})$, with r_o' fixed for all A. Since the radius for ^{58}Ni has a given value for each family regardless of which convention is used, r_o' is determined from the relation $r_o' (58^{1/3} + 6^{1/3}) = r_o\ 58^{1/3}$. The resulting values of V_r and W_S and linear fits are given in Fig. 5. The fits are quite good and should also be good for interpolation and extrapolation.

+ Present Address: Department of Physics and Astronomy, University of Massachusetts, Amherst, Mass. 01002

++ Present Address: Xerox Corporation, Webster, N.Y. 14580

+++ Present Address: IBM Corporation, Rochester, MN 55901

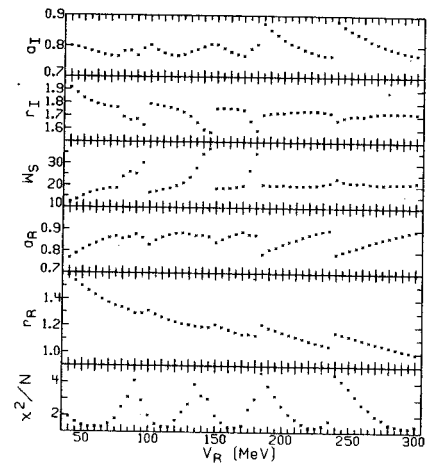

Fig. 1.

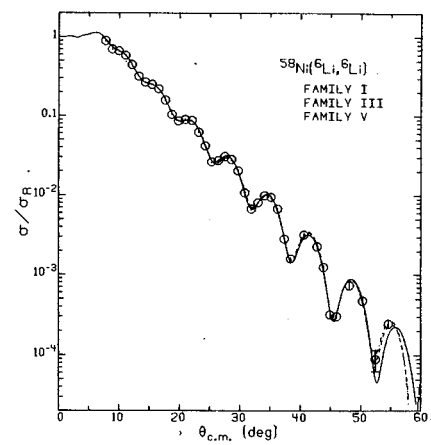

Fig. 2.

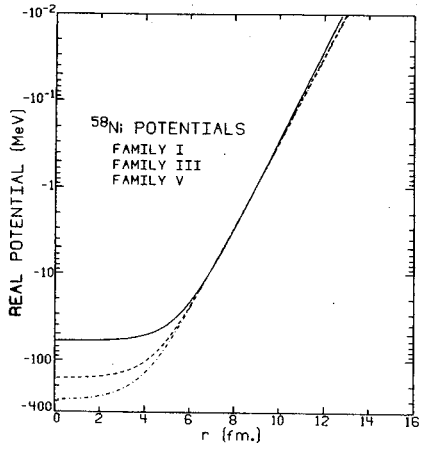

Fig. 3.

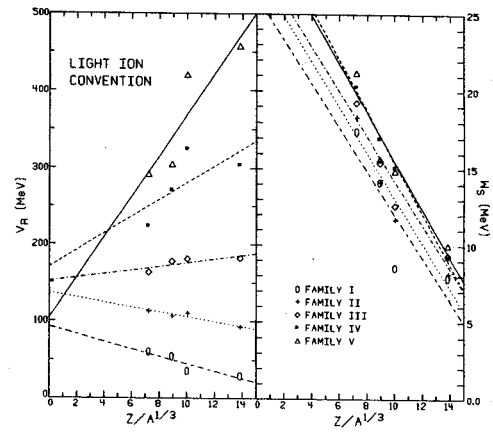

Fig. 4.

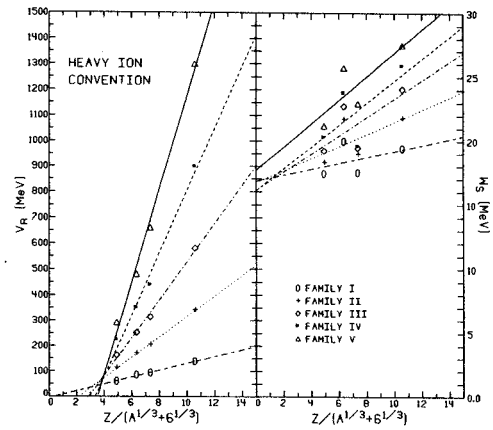

Fig. 5.

Best fit optical model parameters from grids on V_R

Target	Family	V_R (MeV)	r_R (fm)	a_R (fm)	W_s (MeV)	r_I (fm)	a_I (fm)	σ_R (mb)	I_R (MeV)	I_I (MeV)
^{58}Ni	I	60.0	1.431	0.837	17.4	1.787	0.778	2085.	4.49×10^4	1.26×10^5
^{58}Ni	II	111.7	1.258	0.867	18.3	1.768	0.775	2065.	3.05×10^4	1.25×10^5
^{58}Ni	III	163.0	1.161	0.876	19.2	1.753	0.777	2060.	2.75×10^4	1.19×10^5
^{58}Ni	IV	223.4	1.081	0.882	20.3	1.738	0.777	2055.	2.55×10^4	1.16×10^5
^{58}Ni	V	292.0	1.015	0.885	21.2	1.726	0.779	2054	2.47×10^4	1.12×10^5

Inelastic Scattering of ^{6}Li from ^{58}Ni at 71 MeV

C. Williamson*, A. Galonsky, R. Huffman+, and R. Markham++

Nine excited states of ^{58}Ni were studied via the ^{58}Ni(^{6}Li,^{6}Li') reaction at 71.2 MeV. Five sets of optical model parameters for a complex potential of the Woods-Saxon form which gave good fits to the elastic scattering[1] were used to describe the reaction. It was anticipated that comparison of the experimental inelastic angular distributions with the theoretical predictions would produce an unambiguous choice of optical model parameters to describe the elastic scattering process. This was not possible; the five sets of parameters gave equally good fits to the data. Fits for two of the parameter sets are shown in Fig. 1. The solid lines are derived from Family I of Ref. 1 (V_R = real well depth = 60 MeV) and the dashed lines from Family V (V_R = 296 MeV). They give a reasonable fit to the data and they are almost indistinguishable. The DWBA code DWUCK-72[2] was used for these calculations.

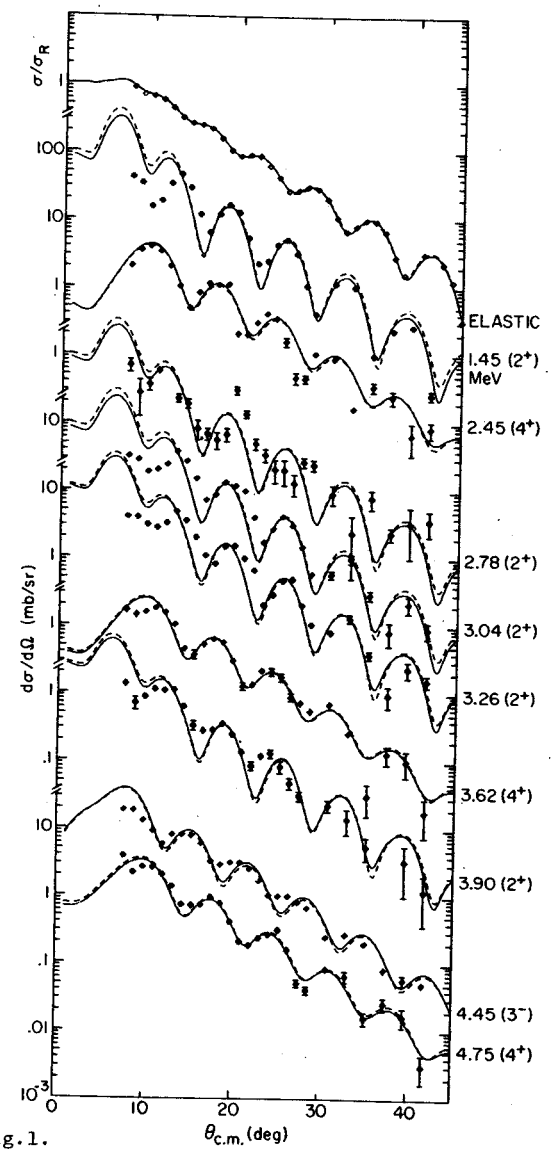

Fig. 1.

The most consistent deficiency of the fits in Fig. 1 is at small angles for the 2^+ states. In an attempt to reduce this deficiency, coupled-channels calculations were performed with the code ECIS[3] for the lowest-energy vibrational band. The ground state, the first 2^+ state (1.45 MeV), and the first 4^+ state (2.46 MeV) were coupled in these calculations. Figure 2 shows the results. The very forward part of the 2^+ angular distribution is, indeed, fitted much better with ECIS than with DWUCK-72. At the larger angles the fit is, however, not quite as good. The ECIS fit to the 4^+ data is also an improvement, since it keeps in phase with the oscillations over the entire angular range of the measurements.

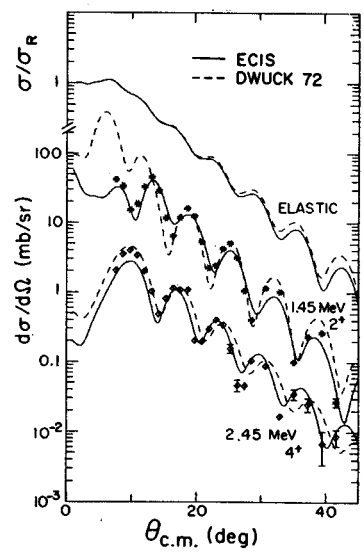

Fig. 2.

Deformation lengths derived from these analyses and from previous analyses of inelastic scattering with particles other than ^{6}Li are presented in Fig. 3. Horizontal bars in this figure represent high, low, and average values of previous analyses. The two squares give the results of the coupled-channels analysis. Triangles result from DWBA analyses in which all parts of the interaction, real, imaginary, and Coulomb, had the same deformation length. (Since the radii for these three parts were not the same, the deformation parameters, β, were all different.) DWBA analyses were also done in which all parts of the potential had the same value of β for a given state. Because the imaginary potential was producing most of the inelastic scattering, the radius of the imaginary well

was used to multiply the β values and yield deformation lengths. These lengths are represented by the circles. There does not seem to be any general conclusion to be drawn from Fig. 3.

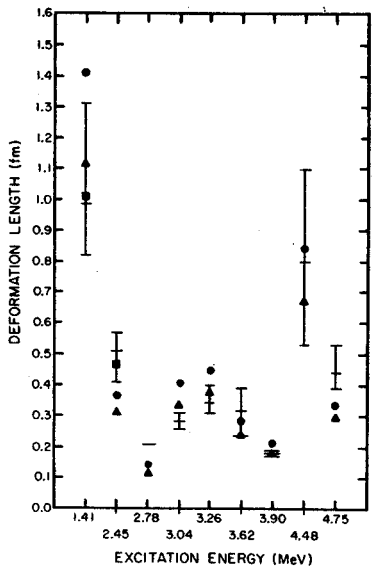

Fig. 3.

---

*Present Address: IBM Corporation, Rochester, MN 55901.

+Present Address: Physics Dept., University of Massachusetts, Amherst. Mass. 01002.

++Present Address: Xerox Corporation, Webster, New York 14580.

1. Elastic Scattering of ^{6}Li at 73.7 MeV, R. Huffman et al., this progress report.

2. P.D. Kunz, University of Colorado, (Unpublished).

3. J. Raynal, Centre d'Etudes Nucleaires de Saclay, (Unpublished).

Optical Model Studies of Neutron Elastic Scattering at 30.3 and 40 MeV

R.P. DeVito, S.M. Austin, W.A. Sterrenburg, U.E.P. Berg

Elastic scattering angular distributions ($15^{o} \leq \theta_{lab} \leq 130^{o}$) scattered from targets of ^{12}C, ^{28}Si, ^{32}S, ^{40}Ca, ^{208}Pb and ^{209}Bi have been measured using the MSU beam swinger TOF system.[1] The $^{7}Li(p,n)^{7}Be$ reaction served as a neutron source. Overall energy resolution was typically 500-1000 keV FWHM. Relative uncertainties are typically < 3% and normalization errors are < 3%. Figures 1 and 2 show the measured angular distribution for 30.3 MeV neutrons on ^{208}Pb and 40 MeV neutrons on ^{32}S respectively, not corrected for multiple scattering, attenuation or finite angle effects. Relative errors are the size of the plotted points or smaller.

Optical model (OM) fits to the data are determined by fitting experimental data with OM cross sections smeared to account for multiple scattering, attenuation and finite angle effects. The line through the data in Figure 1 and in Figure 2 is the fit with a smeared OM cross section. From the final OM fit corrected certer-of-mass cross sections are deduced. Figures 3 and 4 show these cross sections for 30.3 MeV neutrons on ^{208}Pb and 40 MeV neutrons on ^{32}S respectively. The line through the data is the OM prediction for the parameters obtained in the fit of Figures 1 and 2.

The form of the OM potential parametization is the same as that used by Becchetti and Greenless.[2] Since no polarization data are available for neutrons of these energies, the spin-orbit terms are kept fixed at the Becchetti and Greenless best fit value. Each angular distribution is analyzed in terms of potentials where all parameters except spin-orbit were allowed to vary. For ^{40}Ca and ^{208}Pb the data are also analyzed in terms of a potential with fixed geometry.

The isospin dependence of the OM potential is of the form

$$V(r,E)=V_{o}(r,E) + \frac{4}{A}\vec{t}\cdot\vec{T}\,V_{1}(r,E)$$

where $\vec{t}$ is the isospin of the projectile and $\vec{T}$ that of the target. The difference between proton and neutron potentials at the same energy is $V^{(p)}(r,E)-V^{(n)}(r,E)=(2\varepsilon V_{1}(E) + \Delta V_{c})f(r)$, where $\varepsilon \equiv (N-Z)/A$. The potentials for 30.3 and 40 MeV neutrons on ^{40}Ca together with those of Rapaport et al.[3] are compared to proton potentials from the analysis of van Oers.[4] The difference between proton and neutron potentials for N=Z nuclei is just the Coulomb correction term. This term is deduced to be $\Delta V_{c}=0.45\ Z/A^{1/3}$MeV, larger than the value used by Becchetti and Greenless and in good agreement with the value derived by Rapaport et al.[3] using the lower energy neutron data only.

Given the value of ΔV_{c}, the isovector term $V_{1}(E)$ can be deduced by comparing proton and neutron potentials for N≠Z nuclei. This was done for ^{208}Pb using the present data at 30.3 and 40 MeV for neutrons together with the potentials of Rapaport et al.[5] for 7-26 MeV neutron scattering. Comparison is made to the proton potentials given by van Oers et al.[6] An energy dependent value of V_{1} is obtained which when evaluated at 30 MeV is about half that of the Becchetti and Greenless value.

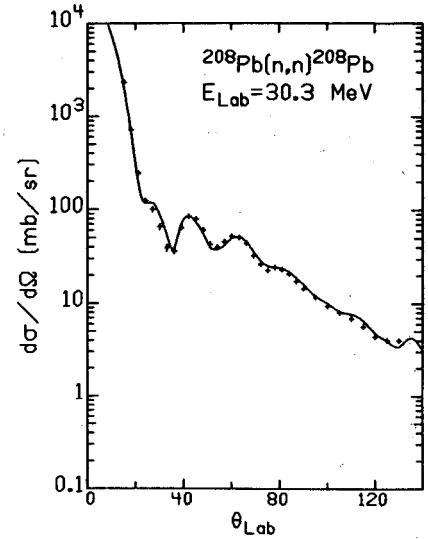

Fig. 1. Measured differential cross section for 30.3 MeV neutrons on ^{208}Pb uncorrected for multiple scattering, attenuation and finite angle effects, and fitted with smeared optical model cross section.

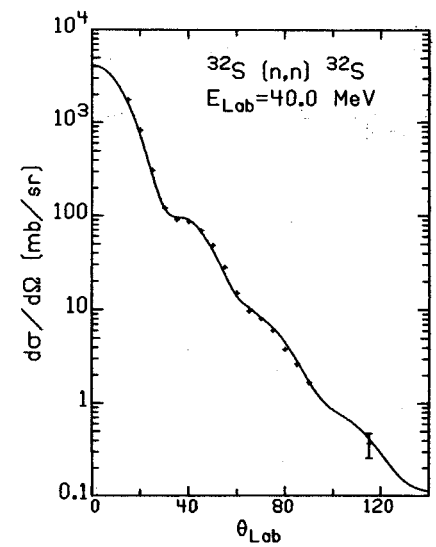

Fig. 2. Same as Figure 1 except for 40 MeV neutrons on ^{32}S.

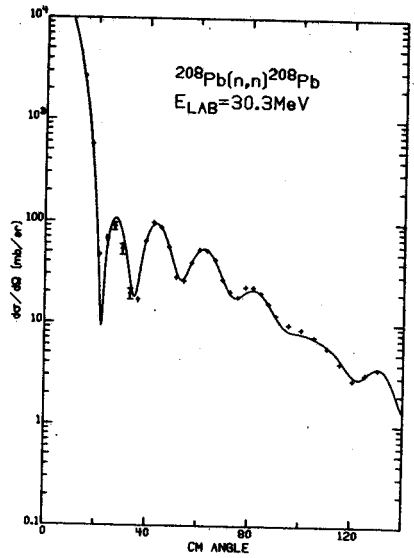

Fig. 3. Corrected center of mass differential cross sections for 30.3 MeV neutrons on ^{208}Pb with optical model fit.

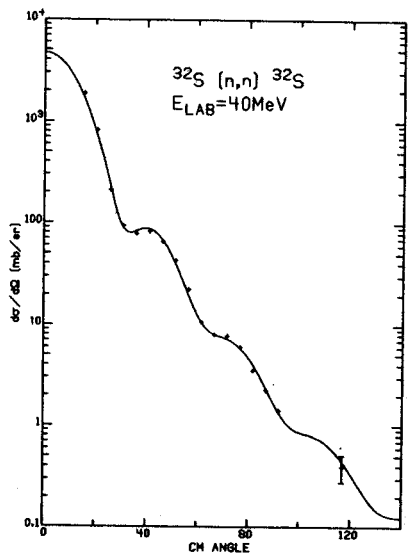

Fig. 4. Same as Figure 3 except for 40 MeV neutrons on ^{32}S.

1. R.K. Bhowmik et al. Nucl. Inst. Meth., 143 (1977) 63.
2. F.D. Becchetti, Jr. and G.W. Greenless, Phys. Rev. 182 (1969) 1190.
3. J. Rapaport et al. Nucl. Phys. A286 (1977) 232.
4. W.T.H. van Oers, Phys. Rev. C3 (1971) 1550.
5. J. Rapaport et al. Nucl. Phys. A296 (1978) 95.
6. W.T.H. van Oers et al. Phys. Rev. C10 (1974) 307.